

Bose-Einstein condensation of photons and grand-canonical condensate fluctuations

Jan Klaers

Institute for Applied Physics, University of Bonn, Germany

Present address:

Institute for Quantum Electronics, ETH Zürich, Switzerland

Martin Weitz

Institute for Applied Physics, University of Bonn, Germany

Abstract

We review recent experiments on the Bose-Einstein condensation of photons in a dye-filled optical microresonator. The most well-known example of a photon gas, photons in blackbody radiation, does not show Bose-Einstein condensation. Instead of massively populating the cavity ground mode, photons vanish in the cavity walls when they are cooled down. The situation is different in an ultrashort optical cavity imprinting a low-frequency cutoff on the photon energy spectrum that is well above the thermal energy. The latter allows for a thermalization process in which both temperature and photon number can be tuned independently of each other or, correspondingly, for a non-vanishing photon chemical potential. We here describe experiments demonstrating the fluorescence-induced thermalization and Bose-Einstein condensation of a two-dimensional photon gas in the dye microcavity. Moreover, recent measurements on the photon statistics of the condensate, showing Bose-Einstein condensation in the grandcanonical ensemble limit, will be reviewed.

1 Introduction

Quantum statistical effects become relevant when a gas of particles is cooled, or its density is increased, to the point where the associated de Broglie wavepackets spatially overlap. For particles with integer spin (bosons), the phenomenon of Bose-Einstein condensation (BEC) then leads to macroscopic occupation of a single quantum state at finite temperatures [1]. Bose-Einstein condensation in the gaseous case was first achieved in 1995 by laser and subsequent evaporative cooling of a dilute cloud of alkali atoms [2–4], as detailed in preceding chapters of this volume. The condensate atoms can be described by a macroscopic single-particle wavefunction, similar as known from liquid helium [1]. Bose-Einstein condensation has also been observed for exciton-polaritons, which are hybrid states of matter

and light [5–7], magnons [8], and other physical systems, see the following chapters of this volume. Other than material particles, photons usually do not show Bose-Einstein condensation [9]. In blackbody radiation, the most common Bose gas, photons at low temperature disappear, instead of condensing to a macroscopically occupied ground state mode. In this system, photons have a vanishing chemical potential, meaning that the number of photons is determined by the available thermal energy and cannot be tuned independently from temperature. Clearly, a precondition for a Bose-Einstein condensation of photons is a thermalization process that allows for an independent adjustment of both photon number and temperature. Early theoretical work has proposed a thermalization mechanism by Compton scattering in plasmas [10]. Chiao et al. proposed a two-dimensional photonic quantum fluid in a nonlinear resonator [11]. Thermal equilibrium here was sought from photon-photon scattering, in analogy to atom-atom scattering in cold atom experiments, but the limited photon-photon interaction in available nonlinear materials has yet prevented a thermalization [12]. In the strong coupling regime, (quasi-)equilibrium Bose-Einstein condensation of exciton-polaritons, mixed states of matter and light, has been achieved [5–7]. Here interparticle interactions of the excitons drive the system into or near thermal equilibrium. More recently, evidence for superfluidity of polaritons has been reported [13,14]. Other experimental work has observed the kinetics of condensation of classical optical waves [15].

Bose-Einstein condensation of photons in a dye filled microresonator has been realized in 2010 in our group at the University of Bonn and in 2014 at Imperial College London [16,17]. Thermalization of the photon gas with the dye solution is achieved by repeated absorption and re-emission processes. For liquid dye solutions at room temperature conditions, it is known that rapid decoherence from frequent collisions (10^{-14} s timescale) with solvent molecules prevent a coherent excitation exchange between photonic and electronic degrees of freedom [18,19], so that the condition of strong light-matter coupling is not met. It is therefore justified to regard the bare photonic and electronic excitations of the system as the true energy eigenstates. The separation between the two curved resonator mirrors, see Fig. 1a, is of order of the photon wavelength. The small cavity spacing causes a large frequency spacing between the longitudinal resonator modes, which is of order of the emission width of the dye molecules, see Fig. 1b. Under these conditions, only photons of a fixed longitudinal mode are observed to populate the resonator, which effectively makes the photon gas two-dimensional as only the two transversal motional degrees of freedom remain. The lowest lying mode of this manifold ($q = 7$), the TEM_{00} transverse ground mode, acts as a low frequency cutoff at an energy of $\hbar\omega_c \simeq 2.1$ eV in the Bonn experiment [16,20]. This restricts the photon spectrum to energies $\hbar\omega$ well above the thermal energy $k_B T \simeq 1/40$ eV, i.e. $\hbar\omega \geq \hbar\omega_c \gg k_B T$, which to good approximation decouples the number of photons from the heat content of the system (non-vanishing chemical potential). In this situation, the photon number becomes tunable by (initial) optical pumping, which can be regarded as fully analogous to the loading of cold atoms into a magnetic or optical dipole trap.

In the microcavity, the energy-momentum relation moreover becomes quadratic, as for a massive particle, and the mirror curvature induces an effective trapping potential in the transverse plane. In general, significant population of high transverse modes ($\text{TEM}_{\alpha\beta}$ with high transversal mode numbers α and β and, correspondingly, high eigenfrequencies) are expected at high temperatures, while the population concentrates to the lowest transverse

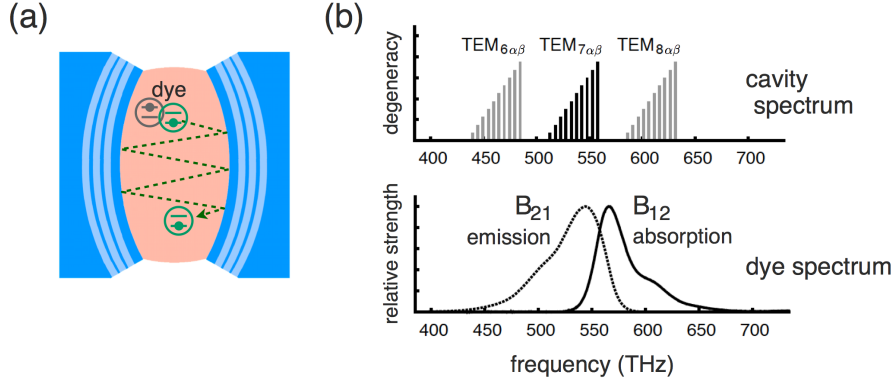


Figure 1 | (a) Scheme of the experimental setup used in [16]. (b) Schematic spectrum of cavity modes. Transverse modes belonging to the manifold of longitudinal mode number $q = 7$ are shown by black lines, those of other longitudinal mode numbers in grey. The bottom graph indicates the relative absorption coefficient and fluorescence strength of rhodamine 6G dye versus frequency.

modes, when the system is cold. One can show that the photon gas in the resonator is formally equivalent to a harmonically trapped two-dimensional gas of massive bosons with effective mass $m_{\text{ph}} = \hbar\omega_c(n/c)^2$. Here c denotes the vacuum speed of light and n the index of refraction of the resonator medium. In thermal equilibrium, such a system is known to undergo Bose-Einstein condensation at a finite temperature [21]. Both the thermalization of the photon gas to room temperature [20] and the Bose-Einstein condensation [16] has been verified experimentally.

Several theoretical publications have discussed different aspects of photon Bose-Einstein condensation using a variety of approaches [22–32], including work based on a superstatistical approach [23], on a Schwinger-Keldysh theory [26], and on a master equation approach [24]. Investigated topics include first-order coherence properties such as the dynamics of phase coherence onset [25], and equilibrium phase fluctuations of the photon condensate [30]. Moreover, second-order coherence properties of photon condensates have been studied in some detail [22, 23, 32]. The coupling of the photon gas to the dye medium, which allows for both energy and particle exchange, can be described by a grand-canonical ensemble representation. This leads to physically observable consequences in the condensed phase regime, in which the condensate performs anomalously large intensity fluctuations [22]. Another key topic is the relation between lasing and condensation. These different regimes have been studied in a theory model accounting for photon loss leading to partial thermal equilibrium of the photon gas [24].

In the following, section 2 gives a theoretical description of the fluorescence induced thermalization mechanism, as well as the expected thermodynamic behavior of the two-dimensional photon gas in the dye-filled microcavity system. Further, section 3 describes experiments observing the thermalization and Bose-Einstein condensation of the photon gas at room temperature. Section 4 reviews theory and experimental results regarding the grand-canonical nature of the condensate fluctuations. Finally, section 5 concludes this contribution.

2 Thermodynamics of a two-dimensional photon gas

2.1 Thermal and chemical equilibrium

In the dye-filled microcavity system, the photon gas in the resonator is thermally coupled to the dye medium. This thermalization mechanism relies on two pre-conditions. First, the dye medium itself has to be in thermal equilibrium. Consider an idealized dye molecule with an electronic ground state and an electronically excited state separated by the energy $\hbar\omega_{\text{ZPL}}$ (zero-phonon-line), each subject to additional rotational and vibrational level splitting [33]. Frequent collisions of solvent molecules with the dye, on the timescale of a few femtoseconds at room temperature, rapidly alter the rovibrational state of the dye molecules. These collisions are many orders of magnitude faster than the electronic processes (the upper state natural lifetime of e.g. rhodamine 6G dye is 4 ns), so that both absorption and emission processes will take place from an equilibrated internal state. One can show that the Einstein coefficients for absorption and emission $B_{12,21}(\omega)$ then will be linked by a Boltzmann factor

$$\frac{B_{21}(\omega)}{B_{12}(\omega)} = \frac{w_{\downarrow}}{w_{\uparrow}} e^{-\frac{\hbar(\omega-\omega_{\text{ZPL}})}{k_{\text{B}}T}}, \quad (1)$$

where $w_{\downarrow,\uparrow}$ are statistical weights related to the rovibrational density of states [22]. This relation is known as the Kennard-Stepanov law [33–38]. Experimentally, the Kennard-Stepanov relation is well fulfilled for many dye molecules. Deviations from this law can either arise from imperfect rovibrational relaxation or a reduced fluorescence quantum yield [39].

The second pre-condition for the light-matter thermalization process is the chemical equilibrium between photon gas and dye medium. Absorption and emission processes can be regarded as a photochemical reaction of the type $\gamma + \downarrow \rightleftharpoons \uparrow$ between photons (γ), excited (\uparrow) and ground state (\downarrow) molecules. This reaction reaches chemical equilibrium, if the rates of competing processes (such as pump and loss) are negligible and there is no net change in the densities of one of the species anymore. The corresponding chemical potentials then satisfy $\mu_{\gamma} + \mu_{\downarrow} = \mu_{\uparrow}$, which can also be expressed as [22]

$$e^{\frac{\mu_{\gamma}}{k_{\text{B}}T}} = \frac{w_{\downarrow}}{w_{\uparrow}} \frac{\rho_{\uparrow}}{\rho_{\downarrow}} e^{\frac{\hbar\omega_{\text{ZPL}}}{k_{\text{B}}T}}, \quad (2)$$

where ρ_{\uparrow} (ρ_{\downarrow}) denotes the density of excited (ground state) molecules. In equilibrium, the photon chemical potential is thus determined by the excitation ratio $\rho_{\uparrow}/\rho_{\downarrow}$ of the medium. Assuming both the Kennard-Stepanov law eq. (1) and chemical equilibrium, as expressed by eq. (2), one can show that multiple absorption-emission cycles drive the photon gas into thermal equilibrium with the dye solution at temperature T , and with a photon chemical potential μ_{γ} determined by the molecular excitation ratio [22].

2.2 Cavity photon dispersion and BEC criticality

The energy of a cavity photon is determined by its longitudinal (k_z) and transversal wavenumber (k_r) as $E = (\hbar c/n)\sqrt{k_z^2 + k_r^2}$, where n again denotes the index of refraction of the medium. Owing to the curvature of the mirrors, the boundary conditions for the photon

field depend on the distance to the optical axis $r = |\mathbf{r}|$. For the longitudinal component, we set $k_z(\mathbf{r}) = q\pi/D(r)$ where q denotes the longitudinal mode number and $D(r)$ describes the mirror separation as a function of r . For a symmetric resonator consisting of two spherically curved mirror with separation D_0 and radius of curvature R , in a paraxial approximation ($r \ll R$, $k_r \ll k_z$), the photon energy is given by [20]

$$E \simeq m_{\text{ph}}(c/n)^2 + \frac{(\hbar k_r)^2}{2m_{\text{ph}}} + \frac{1}{2}m_{\text{ph}}\Omega^2 r^2, \quad (3)$$

with an effective photon mass $m_{\text{ph}} = \pi\hbar nq/cD_0$ and trapping frequency $\Omega = c/n\sqrt{D_0R/2}$. This describes a particle moving in the two-dimensional transversal plane with non-vanishing (effective) mass subject to a harmonic trapping potential with trapping frequency Ω . Such a system is known to undergo Bose-Einstein condensation at finite temperature [21]. If we account for the two-fold polarization degeneracy of photons, condensation is expected, when the particle number exceeds the critical particle number

$$N_c = \frac{\pi^2}{3} \left(\frac{k_B T}{\hbar\Omega} \right)^2. \quad (4)$$

The typical trapping frequency in our setup is $\Omega/2\pi \simeq 41$ GHz, and at room temperature ($T = 300$ K) one obtains a critical photon number of $N_c \simeq 77,000$, which is experimentally feasible. The physical reason for the possibility to observe Bose-Einstein condensation at room temperature conditions is the small effective photon mass $m_{\text{ph}} = \hbar\omega_c(n/c)^2 \simeq 7 \cdot 10^{-36}$ kg, which is ten orders of magnitude smaller than e.g. the mass of the rubidium atom.

2.3 Equilibrium versus non-equilibrium

In general, particle loss can drive a system out of equilibrium, if the timescale associated to loss is not well separated from the timescale for the equilibration of the system. Separated timescales clearly can be achieved for the case of dilute atomic gases. The true ground state for e.g. an atomic rubidium gas is a cloud of molecular dimers. However, researchers have learned in the 1980's to the early 1990's that the recombination rate from three-body collisions to the molecular state can be kept sufficiently small by the use of very dilute atomic clouds for which the corresponding rates are sufficiently small [40, 41]. High phase space densities can nevertheless be achieved by cooling to ultralow temperatures in the nano-Kelvin regime. Correspondingly, quantum degeneracy of a cloud of bosonic atoms can be reached under conditions that are close to equilibrium.

In the case of photons, non-equilibrium conditions can either arise from a violation of the Kennard-Stepanov law (eq. 1) or from a violation of chemical equilibrium (eq. 2), if e.g. the photon loss rate is not negligible compared to the photon absorption and emission rate. Clearly, the latter situation is well known from typical laser operation. Both laser operation and Bose-Einstein condensation, either of photons or atoms [42], rely on Bose-enhancement. However, to achieve lasing at the desired wavelength, it is usually necessary to break the chemical equilibrium between photons and molecules, allowing for a departure from Bose-Einstein statistics and for a photon energy distribution independent of energetics. For this

purpose, gain and loss are deliberately engineered, for example, by frequency-selective components. In the field of exciton-polaritons, the question whether a system that is pumped and exhibits losses should be regarded as polariton laser or polariton Bose-Einstein condensate has been extensively discussed [43–45], see also following articles in this volume. For the case of photonic Bose-Einstein condensation, the role of losses and pumping has been theoretically investigated by Kirton and Keeling [24]. Experimentally, the crossover between equilibrium and non-equilibrium photon gases has been studied both in the non-degenerate and in the quantum degenerate regime [17, 20, 46].

3 Experiments on photon condensation

A scheme of the setup used in the Bonn photon condensation experiment is shown in Fig. 1a. The optical resonator consists of two highly reflecting spherically curved mirrors ($\simeq 0.999985$ reflectivity in the relevant wavelength region) with radius of curvature $R = 1$ m. One of mirrors is cut to $\simeq 1$ mm surface diameter to allow for a cavity length in the micrometer range ($D_0 \simeq 1.46 \mu\text{m}$), as measured by the cavity free spectral range, despite the mirror curvature. The resonator contains a drop of liquid dye, typically rhodamine 6G or perylenedimide (PDI), solved in an organic solvent. Both of these dyes have high quantum efficiencies between 0.95 and 0.97, and fulfill the Kennard-Stepanov relation in good approximation. Fig. 1b shows the cavity spectrum (top) along with the absorption and fluorescence spectrum for rhodamine dye (bottom). The resonator setup is off-resonantly pumped with a laser beam near 532 nm wavelength derived from a frequency doubled Nd:YAG laser inclined under 45° angle to the cavity axis.

In initial experiments, the thermalization of the two-dimensional photon gas in the dye-filled microresonator was carefully tested [20]. Fig. 2a shows experimental spectra of the light transmitted through one cavity mirror for two different temperatures of the setup (top: $T \simeq 300$ K, room temperature; bottom $T \simeq 365$ K). In these experiments, the average photon number inside the cavity ($N \simeq 50$) is three orders of magnitude below the critical particle number. The experimental data (dots) in both cases is well described by a Boltzmann distribution of photon energies at the corresponding temperature (solid line). In other experiments, the pump spot was transversely displaced by a variable amount and the position where the maximum of the observed fluorescence occurs was monitored, see Fig. 2b. As expected in the presence of a trapping potential, a spatial relaxation of the photons towards regions of low potential energy near the optical axis was observed.

In subsequent experiments, the dye-filled microcavity was operated at photon numbers sufficiently high to reach quantum degeneracy. To avoid excessive population of dye molecules in triplet states and heat deposition, the optical pump beam was acousto-optically chopped to $0.5 \mu\text{s}$ long pulses, with a 8 ms repetition time. Fig. 3a shows typical spectra of the photon gas at different photon numbers [16]. While the observed spectrum resembles a Boltzmann-distribution at small intracavity optical powers, near the phase transition a shift of the maximum towards the cutoff frequency is observed, and the spectrum more resembles a Bose-Einstein distribution. At intracavity powers above the critical value, the Bose-Einstein condensate occurs as a spectrally sharp peak at the position of the cutoff. The observed spectral width of the condensate peak is limited by the resolution of the used spectrometer.

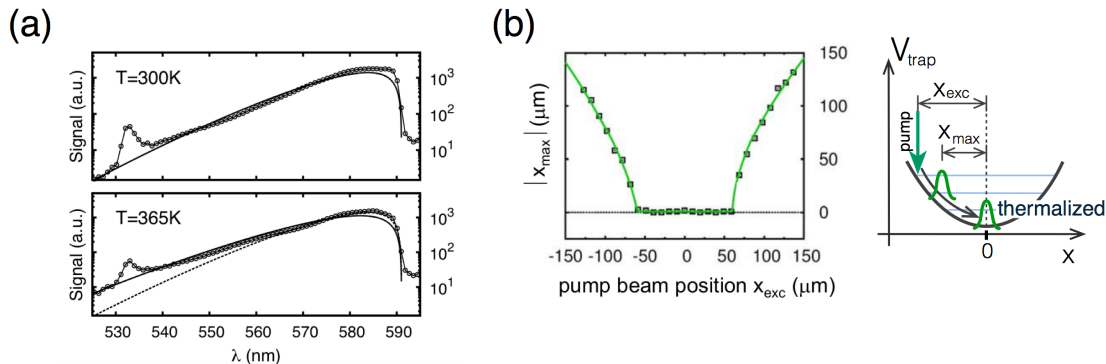


Figure 2 | (a) Measured spectral intensity distributions (connected dots) of the cavity emission for temperatures of the resonator setup of 300 K (top) and 365 K (bottom) at an average photon number of 60 ± 10 inside the cavity, i.e. far below the onset of a BEC. The solid lines are theoretical spectra based on a Bose-Einstein distribution. For illustration a $T = 300\text{K}$ distribution is also inserted in the bottom graph (dashed line). (b) Distance of the fluorescence intensity maximum from the optical axis $|x_{\max}|$ versus transverse position of the pump spot, x_{exc} . Due to the thermalization, the photon gas accumulates in the trap center, where the potential exhibits a minimum value. This holds as long as the excitation spot is closer than approximately $60\ \mu\text{m}$ distance. Figure taken from Ref. [20].

The experimental results are in good agreement with theoretical expectations (see the inset of the figure). At the phase transition, the optical intracavity power is $P_{\text{c,exp}} = (1.55 \pm 0.6)\text{ W}$, which corresponds to a photon number of $(6.3 \pm 2.4) \cdot 10^4$.

Fig. 3b shows spatial images of the light transmitted through one of the cavity mirrors (real image onto a color CCD camera) both below (top) and above (bottom) the condensate threshold. Both images show a shift from the yellow spectral regime for the transversally low excited cavity modes located near the trap center to the green for transversally higher excited modes appearing at the outer trap regions. In the lower image, a bright spot is visible in the center with a measured FWHM diameter of $(14 \pm 2)\ \mu\text{m}$. Within the quoted experimental uncertainties, this corresponds well to the expected diameter of the TEM_{00} transverse ground state mode of $12.2\ \mu\text{m}$, yielding clear evidence for a single-mode macroscopic population of the ground state. Fig. 3c gives normalized intensity profiles (cuts along one axis through the trap center) for different powers. One observes that not only the height of the condensate peak increases for larger condensate fractions, but also its width, see also Fig. 3d. This effect is not expected for an ideal photon gas, and suggests a weak repulsive self-interaction mediated by the dye solution. The origin of the self-interaction is thermal lensing, which under steady state conditions can be described by a non-linear term analogous to the Gross-Pitaevskii equation (see [16]). In general, the interplay between optical and heat flow equations can lead to non-local interactions, see [29]. By comparing the observed increase of the mode diameter with numerical solutions of the two-dimensional Gross-Pitaevskii equation, a dimensionless interaction parameter was estimated [16]. This interaction parameter is found to be significantly smaller than the values reported for two-dimensional atomic physics quantum gas experiments [47,48] and also below the values at which Kosterlitz-Thouless physics can be

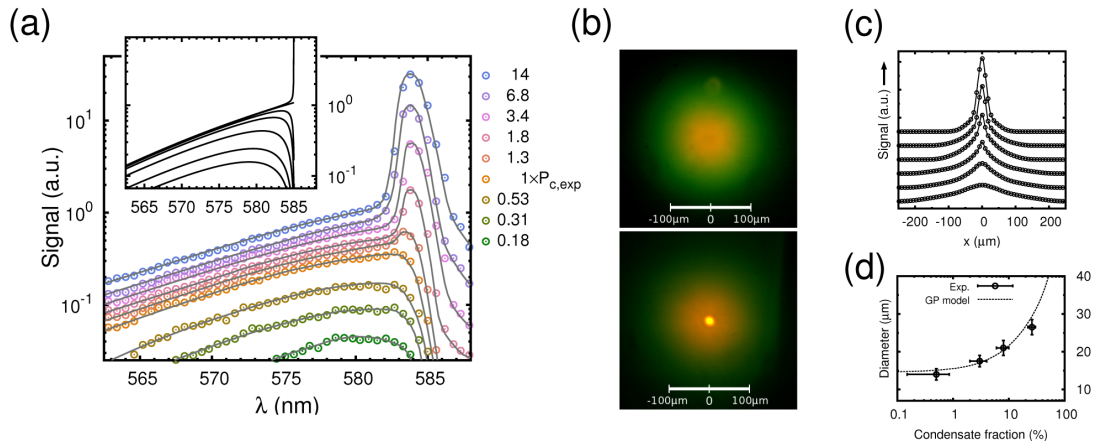


Figure 3 | (a) The connected circles show measured spectral intensity distributions for different pump powers. The legend gives the optical intracavity power, determining the photon number. On top of a broad thermal wing, a spectrally sharp condensate peak at the position of the cavity cutoff is visible above a critical power. The observed peak width is limited by the spectrometer resolution. The inset gives theoretical spectra based on Bose-Einstein distributed transversal excitations. (b) Images of the radiation emitted along the cavity axis, below (top) and above (bottom) the critical power. In the latter case, a condensate peak is visible in the center. (c) Cuts through the center of the observed intensity distribution for increasing optical pump powers. (d) The data points give the measured width of the condensate peak versus condensate fraction and the dotted line is the result of a theoretical model based on the Gross-Pitaevskii equation. Figure taken from Ref. [16].

expected to become important in the harmonically trapped case [49]. Experimentally, when directing the condensate through a Michelson-type sheering interferometry, no signatures of phase blurring (that occur in two-dimensional atomic gas experiments) were observed [50]. Further signatures consistent within the framework of Bose-Einstein condensation include the expected scaling of the critical photon number with resonator geometry, and a spatial relaxation process that leads to a strongly populated ground mode even for a spatially displaced pump spot [16].

4 Fluctuations of photon condensates

4.1 Photon condensates coupled to a particle reservoir

In this section, we discuss quantum statistical properties of photon condensates, in particular the photon number distribution and particle number fluctuations. The main result is that photon Bose-Einstein condensates in the dye microcavity system, owing to the grand-canonical nature of the light-matter thermalization process, can show unusually large particle number fluctuations, which are not observed in present atomic Bose-Einstein condensates.

In statistical physics, different statistical ensembles reflect different laws of conservation that can be realized in experiments. The micro-canonical ensemble corresponds to a physical system with energy and particle number strictly fixed at all times, while in the canonical

ensemble energy fluctuates around a mean value determined by the temperature of a heat reservoir. Under grand-canonical conditions, both an exchange of energy and particles with a large reservoir is allowed leading to fluctuations in both quantities. The here investigated photon gas in the dye microcavity, with photons being frequently absorbed and emitted by dye molecules, belongs the latter class of experiments. As discussed in section 2, absorption and emission can be regarded as the two directions of a photochemical reaction $\gamma + \downarrow \rightleftharpoons \uparrow$, where photons (γ), ground state (\downarrow) and excited dye molecules (\uparrow) are repeatedly converted into each other, and the dye molecules act as a “reservoir species” for the photon gas.

A common assumption is that the ensemble conditions realized in a physical system are not essential for its physical behavior. The various statistical approaches are correspondingly expected to become interchangeable in the thermodynamic limit [9, 51], in the sense that relative fluctuations vanish in all of them, i.e. $\delta N/N \rightarrow 0$ for the average total particle number N and its root mean square deviation δN . This assumption is however violated in the grand-canonical treatment of the ideal Bose gas, where the occupation of any single particle state undergoes relative fluctuations of 100% of the average value [52, 53]. For a macroscopically occupied ground state of a Bose-Einstein condensed gas, this implies fluctuations of order of the total particle number, i.e. $\delta N \simeq N$. While one usually expects fluctuations to freeze out at low temperatures, here the reverse situation is encountered: the total particle number starts to strongly fluctuate as the condensate fraction approaches unity, a behavior that has been recognized early in BEC theory [54] and later has been termed “grand-canonical fluctuation catastrophe” [53, 55, 56]. In experiments with cold atoms, this anomaly has not been observed so far, as sufficiently large particle reservoirs are usually not experimentally realizable. For those systems, much theoretical work has been performed to obtain the particle number fluctuations in a (micro-)canonical description [55, 57–59], and accounting for trapping potentials [60, 61]. A review can be found in reference [53]. Noteworthy, the micro-canonical ensemble description of the ideal Bose gas shows interesting connections to the partitioning and factorizing problem of integer numbers [62].

For a photon Bose-Einstein condensate, grand-canonical ensemble conditions can be an inherent feature of the thermalization process and can therefore influence the second order coherence properties [22]. We consider a situation in which the photon condensate is coupled to the electronic transitions of M dye molecules (located in the volume of the electromagnetic ground mode) by absorption and emissions processes. In this way, the condensate exchanges excitations with a reservoir of a given (finite) size. Using a master equation approach one can show that the probability \mathcal{P}_n to find n photons in the ground state follows

$$\frac{\mathcal{P}_n}{\mathcal{P}_0} = \frac{(M - X)! X!}{(M - X + n)! (X - n)!} e^{-n\hbar(\omega_c - \omega_{\text{ZPL}})/k_{\text{B}}T}, \quad (5)$$

where the excitation number X is defined as the sum of ground mode photon number and electronically excited molecules in the reservoir. As before, ω_c and ω_{ZPL} denote the frequencies of the condensate mode and zero-phonon-line of the medium, respectively. In this calculation, X is constant, i.e. it is not expected to perform large fluctuations on its own. The photon number distribution, which can also be derived in a superstatistical approach [23], in general interpolates between Bose-Einstein statistics and Poisson statistics. Assuming that the excitation level $\rho_{\uparrow}/\rho_{\downarrow} \simeq X/(M - X)$ of the medium stays fixed, which conserves the

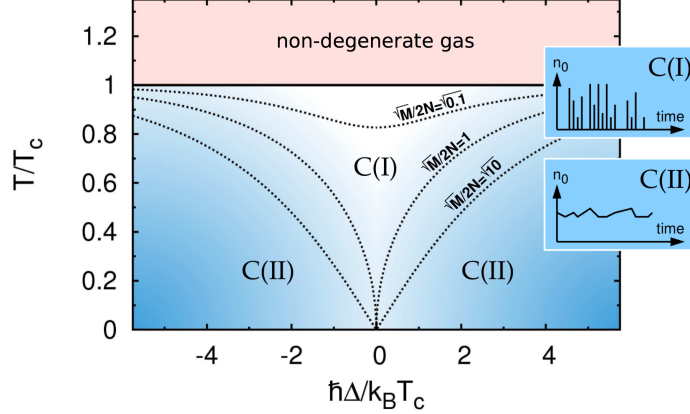


Figure 4 | Phase diagram of the two-dimensional photon gas for fixed average photon number \bar{N} in the plane spanned by the reduced temperature T/T_c and the dye-cavity detuning $\hbar\Delta/k_B T_c$. The solid line marks the BEC phase transition. The dashed lines (three cases are shown) separate two regimes: a condensate regime with large number fluctuations and a Bose-Einstein-like photon number distribution C(I), and a regime of non-fluctuating condensates obeying Poisson statistics C(II). The temperature of the crossover C(I)-C(II) depends on the ratio \sqrt{M}/\bar{N} , where the reservoir size M denotes the number of dye molecules in the mode volume of the ground state. The insets give a sketch of the corresponding temporal evolution of the condensate photon number $n_0(t)$. Figure taken from Ref. [22].

chemical potential μ (eq. 2), the average condensate number \bar{n}_0 and total particle number \bar{N} , one finds that large reservoirs M lead to Bose-Einstein-like statistics with an exponentially decaying photon number distribution starting at a maximum value for zero photon number $n = 0$. For small reservoirs \mathcal{P}_n becomes poissonian with a maximum value at a non-zero photon number. The distinction between these two statistical regimes is not unambiguous due to the smooth crossover behavior between them. A natural choice for a borderline is the point at which 'finding zero photons' ceases to be the most probable event, which occurs at $\mathcal{P}_0 = \mathcal{P}_1$ and resembles a common laser threshold definition [63]. For the temperature T_x at which this condition is reached, given a certain system size \bar{N} (average photon number) and the reservoir size M , one obtains the equation

$$\bar{N} - \frac{\pi}{6} \left(\frac{k_B T_x}{\hbar\Omega} \right)^2 \simeq \sqrt{\frac{M/2}{1 + \cosh \frac{\hbar\Delta}{k_B T_x}}}. \quad (6)$$

Here Δ denotes the detuning between condensate mode and zero-phonon-line of the dye, defined as $\Delta = \omega_c - \omega_{\text{ZPL}}$. For zero dye-cavity detuning $\Delta = 0$, one finds the analytic solution $T_{x,\Delta=0} \simeq T_c \sqrt{1 - \sqrt{M}/2\bar{N}}$, provided that $\sqrt{M}/2\bar{N} < 1$. For general detunings Δ , equation (6) has to be solved numerically. Figure (4.1) gives a phase diagram, where solutions for three different cases $\sqrt{M}/2\bar{N} = \sqrt{0.1}, 1, \sqrt{10}$ are marked as dashed lines, which separates two different regimes of the photon condensate, denoted by C(I) with Bose-Einstein-like photon statistics and C(II) with Poisson statistics, respectively. In terms of second order correlations, the dashed lines correspond to $g^{(2)}(0) \simeq \pi/2$, or relative fluctuations of $\delta n/\bar{n}_0 = \sqrt{g^{(2)}(0) - 1} = 0.75$. Note that both T_c and T_x are conserved in a thermodynamic

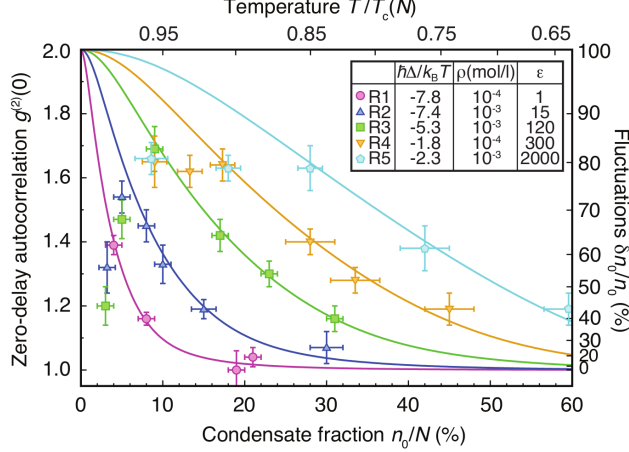


Figure 5 | Zero-delay autocorrelations $g^{(2)}(0)$ and condensate fluctuations $\delta n_0/\bar{n}_0$ versus condensate fraction \bar{n}_0/\bar{N} [or equivalently the corresponding reduced temperature $T/T_c(\bar{N})$ at $T = 300$ K], for five different reservoirs R1-R5. The increase of the effective molecular reservoir size from R1 to R5 is quantified by the parameter ϵ (third column), defined in equation (8). Condensate fluctuations extend deep into the condensed phase for high dye concentration ρ and small dye-cavity detuning Δ (R5). Results of a theoretical model based on equation (5) are shown as solid lines. The error bars indicate statistical uncertainties. Experimental parameters: condensate wavelength $\lambda_0 = \{598, 595, 580, 598, 602\}$ nm for data sets R1-R5; dye concentration $\rho = \{10^{-4}, 10^{-3}, 10^{-3}\}$ mol/l for R1-R3 (rhodamine 6G), and $\rho = \{10^{-4}, 10^{-3}\}$ mol/l for R4-R5 (perylene red). For the theory curves, we find effective reservoir sized of $M = \{5.5 \pm 2.2, 20 \pm 7, 16 \pm 6, 2.1 \pm 0.4, 11 \pm 4\} \times 10^9$ for R1-R5. Figure taken from Ref. [64].

limit $\bar{N}, M, R \rightarrow \infty$ in which $\bar{N}/R = \text{const}$ and $\sqrt{M}/\bar{N} = \text{const}$. A recent theory work has investigated the possible effects of fast photon-photon interactions on the photon number statistics [32].

4.2 Observation of anomalous condensate fluctuations

The intensity correlations and fluctuations of the condensate have been measured using a Hanbury Brown-Twiss setup [64, 65]. In this experiment, the condensate mode is separated from the higher transversal modes by spatial filtering in the far field, which corresponds to a transverse momentum filter. The beam is split into two paths, each of which are directed onto single-photon avalanche photodiodes. Time correlations of the condensate population can be determined with a temporal resolution of 60ps with this setup. The second-order correlation function $g^{(2)}(t_1, t_2) = \langle n_0(t_1)n_0(t_2) \rangle / \langle n_0(t_1) \rangle \langle n_0(t_2) \rangle$ to good approximation is found to depend only on the time delay $\tau = t_2 - t_1$. Further analysis is thus performed with the time averaged function $g^{(2)}(\tau) = \langle g^{(2)}(t_1, t_2) \rangle_{\tau=t_2-t_1}$.

We have varied the reservoir size systematically to test for the grand-canonical nature of the system. Figure (4.2) shows the zero-delay correlations $g^{(2)}(0)$ as a function of the condensate fraction \bar{n}_0/\bar{N} for five combinations of dye concentration ρ and dye-cavity detuning Δ . The data sets labelled with R1-R3 have been obtained with rhodamine 6G

dye ($\omega_{\text{ZPL}} = 2\pi c/545\text{nm}$). For measurements R4 and R5, we have used perylene red ($\omega_{\text{ZPL}} = 2\pi c/585\text{nm}$) as dye species, which allows us to reduce the detuning between condensate and dye reservoir and to effectively increase the reservoir size. Following equation (6), this effective reservoir size can be quantified as

$$M_{\text{eff}} = \frac{M/2}{1 + \cosh(\hbar\Delta/k_{\text{B}}T)}. \quad (7)$$

Furthermore, a relative reservoir size is obtained by normalizing to the reservoir size in measurement R1

$$\epsilon = \frac{M_{\text{eff},R_i}}{M_{\text{eff},R1}} = \frac{\rho_{R_i}}{\rho_{R1}} \times \frac{1 + \cosh(\hbar\Delta_{R1}/k_{\text{B}}T)}{1 + \cosh(\hbar\Delta_{R_i}/k_{\text{B}}T)}. \quad (8)$$

For the lowest dye concentration and largest detuning (R1, $\epsilon = 1$), the particle reservoir is so small that the condensate fluctuations are damped almost directly above the condensation threshold ($\bar{N} \geq N_c$). By increasing dye concentration and decreasing the dye-cavity detuning one can systematically extend the regime of large fluctuations to higher condensate fractions (R1-R5). Our experimental results are recovered by a theoretical modeling shown as solid lines in figure (4.2), except for small condensate fractions below 5%. The here visible drop-off in the correlation signal is attributed to imperfect mode filtering, which does not fully preclude photons in higher transversal cavity modes that are statistically uncorrelated to the ground mode photons from reaching the avalanche photo detectors. The maximum observed zero-delay autocorrelation is $g^{(2)}(0) \simeq 1.67$, corresponding to relative fluctuations of $\delta n_0/\bar{n}_0 = 82\%$, which is slightly less than theoretically expected. For the largest reservoir realized (R5, $\epsilon = 2000$), we observe zero-delay correlations of $g^{(2)}(0) \simeq 1.2$ at a condensate fraction of $\bar{n}_0/\bar{N} \simeq 0.6$. At this point, the condensate still performs large relative fluctuations of $\delta n_0/\bar{n}_0 = \sqrt{g^{(2)}(0) - 1} \simeq 45\%$, although its occupation number is comparable to the total photon number. This clearly demonstrates that the observed super-Poissonian photon statistics is determined by the grand-canonical particle exchange between condensate and dye reservoir.

5 Conclusions

We have described recent experiments on photon Bose-Einstein condensation in a dye-filled optical microresonator. Thermalization of the photon gas is achieved by a fluorescence induced thermalization mechanism, which establishes a thermal contact to the room temperature dye medium, and allows for a freely adjustable chemical potential. The photons here act like a gas of material particles with a phase transition temperature that is many orders of magnitude higher than for dilute atomic Bose-Einstein condensates. A further notable system property is a regime with unconventional fluctuation properties, in which statistical fluctuations of the condensate number comparable to the total particle number occur. This is a yet unexplored regime of Bose-Einstein condensation that originates from the grand-canonical nature of the light-matter thermalization process and breaks the usual assumption of ensemble equivalence in statistical physics. Moreover, the unconventional second order coherence properties of a photon condensate can draw a further borderline (in addition to

the equilibrated system state) to laser-like behavior, if one follows the usual definition of a laser as a both first and second order coherent light source.

For the future, it will be interesting to test for the first order coherence of photon condensation in the grand-canonical limit, and to verify whether such a condensate exhibits superfluidity. A further fascinating perspective is the exploration of periodic potentials for the photon gas, which may allow to tailor novel quantum manybody states of light.

We acknowledge funding from the ERC (INPEC) and the DFG (We 1748-17).

References

- [1] A. J. Leggett, Quantum liquids, Oxford University Press, Oxford; New York (2006).
- [2] M. H. Anderson, J. R. Ensher, M. R. Matthews, C. E. Wieman and E. A. Cornell, Observation of Bose-Einstein condensation in a dilute atomic vapor, *Science* **269**, 198 (1995).
- [3] K. B. Davis, M.-O. Mewes, M. R. Andrews, N. J. van Druten, D. M. Durfee, D. M. Kurn and W. Ketterle, Bose-Einstein condensation in a gas of sodium atoms, *Phys. Rev. Lett.* **75**, 3969 (1995).
- [4] C. C. Bradley, C. A. Sackett and R. G. Hulet, Bose-Einstein condensation of lithium: Observation of limited condensate number, *Phys. Rev. Lett.* **78**, 985 (1997).
- [5] H. Deng, G. Weihs, C. Santori, J. Bloch and Y. Yamamoto, Condensation of semiconductor microcavity exciton polaritons, *Science* **298**, 199 (2002).
- [6] J. Kasprzak, M. Richard, S. Kundermann, A. Baas, P. Jeambrun, J. M. J. Keeling, F. M. Marchetti, M. H. Szymanska, R. Andre, J. L. Staehli, V. Savona, P. B. Littlewood, B. Deveaud and L.S. Dang, Bose-Einstein condensation of exciton polaritons, *Nature* **443**, 409 (2006).
- [7] R. Balili, V. Hartwell, D. Snoke and L. Pfeiffer, Bose-Einstein condensation of microcavity polaritons in a trap, *Science* **316**, 1007 (2007).
- [8] S. O. Demokritov, V. E. Demidov, O. Dzyapko, G. A. Melkov, A. A. Serga, B. Hillebrands and A. N. Slavin, Bose-Einstein condensation of quasi-equilibrium magnons at room temperature under pumping, *Nature* **443**, 430 (2006).
- [9] K. Huang, Statistical Mechanics, Wiley, New York (1987).
- [10] Y. B. Zel'dovich and E. V. Levich, Bose condensation and shock waves in photon spectra, *Sov. Phys. JETP* **28**, 1287 (1969).
- [11] R. Y. Chiao, Bogoliubov dispersion relation for a 'photon fluid': Is this a superfluid?, *Opt. Commun.* **179**, 157 (2000).
- [12] M. W. Mitchell, C. I. Hancox and R. Y. Chiao, Dynamics of atom-mediated photon-photon scattering, *Phys. Rev. A* **62**, 043819 (2000).
- [13] A. Amo, D. Sanvitto, F.P. Laussy, D. Ballarini, E. Del Valle, M.D. Martin, A. Lemaitre, J. Bloch, D.N. Krizhanovskii, M.S. Skolnick, Tejedor C. and Vina L., Collective fluid dynamics of a polariton condensate in a semiconductor microcavity, *Nature* **457**, 291 (2009).
- [14] A. Amo, J. Lefrère, S. Pigeon, C. Adrados, C. Ciuti, I. Carusotto, R. Houdré, E. Giacobino and A. Bramati, Superfluidity of polaritons in semiconductor microcavities, *Nat. Phys.* **5**, 805 (2009).

- [15] C. Sun, S. Jia, C. Barsi, S. Rica, A. Picozzi and J.W. Fleischer, Observation of the kinetic condensation of classical waves, *Nature Phys.* **8**, 470 (2012).
- [16] J. Klaers, J. Schmitt, F. Vewinger and M. Weitz, Bose-Einstein condensation of photons in an optical microcavity, *Nature* **468**, 545 (2010).
- [17] J. Marelic and R. A. Nyman, Experimental evidence for inhomogeneous-pumping and energy-dependent effects in photon Bose-Einstein condensation, *Phys. Rev. A* **468**, 033813 (2015).
- [18] E. De Angelis, F. De Martini and P. Mataloni, Microcavity quantum superradiance, *J. Opt. B - Quantum S. O.* **2**, 149 (2000).
- [19] H. Yokoyama and S. D. Brorson, Rate equation analysis of microcavity lasers, *J. Appl. Phys.* **66**, 4801 (1989).
- [20] J. Klaers, F. Vewinger and M. Weitz, Thermalization of a two-dimensional photonic gas in a ‘white-wall’ photon box, *Nat. Phys.* **6**, 512 (2010).
- [21] V. Bagnato and D. Kleppner, Bose-Einstein condensation in low-dimensional traps, *Phys. Rev. A* **44**, 7439 (1991).
- [22] J. Klaers, J. Schmitt, T. Damm, F. Vewinger and M. Weitz, Statistical physics of Bose-condensed light in a dye microcavity, *Phys. Rev. Lett* **108**, 160403 (2012).
- [23] D. N. Sob’yanin, Hierarchical maximum entropy principle for generalized superstatistical systems and Bose-Einstein condensation of light, *Phys. Rev. E* **85**, 061120 (2012).
- [24] P. Kirton and J. Keeling, Nonequilibrium model of photon condensation, *Phys. Rev. Lett.* **111**, 100404 (2013).
- [25] D. W. Snoke and S. M. Girvin, Dynamics of phase coherence onset in Bose condensates of photons by incoherent phonon emission, *J. Low Temp. Phys.* **171**, 1 (2013).
- [26] A.-W. de Leeuw and H.T.C. Stoof R.A. Duine, Schwinger-Keldysh theory for Bose-Einstein condensation of photons in a dye-filled optical microcavity, *Phys. Rev. A* **88**, 033829 (2013).
- [27] R. A. Nyman and M. H. Szymańska, Interactions in dye-microcavity photon condensates and the prospects for their observation, *Phys. Rev. A* **89**, 033844 (2014).
- [28] A. Kruchkov, Bose-Einstein condensation of light in a cavity, *Phys. Rev. A* **89**, 033862 (2014).
- [29] M. C. Strinati and C. Conti, Bose-Einstein condensation of photons with nonlocal nonlinearity in a dye-doped graded-index microcavity, *Phys. Rev. A* **90**, 043853 (2014).
- [30] A.-W. de Leeuw, E. C. I. van der Wurff, R. A. Duine and H. T. C. Stoof, Phase diffusion in a Bose-Einstein condensate of light, *Phys. Rev. A* **90**, 043627 (2014).
- [31] E. Sela, A. Rosch and V. Fleurov, Condensation of photons coupled to a dicke field in an optical microcavity, *Phys. Rev. A* **89**, 043844 (2014).
- [32] E.C.I. van der Wurff, A.-W. de Leeuw, R.A. Duine and H.T.C. Stoof, Interaction effects on number fluctuations in a Bose-Einstein condensate of light, *Phys. Rev. Lett.* **113**, 135301 (2014).
- [33] J. R. Lakowicz, Principles of fluorescence spectroscopy, Kluwer Academic, New York (1999).
- [34] E. H. Kennard, On the thermodynamics of fluorescence, *Phys. Rev.* **11**, 29 (1918).
- [35] E. H. Kennard, The excitation of fluorescence in fluorescein, *Phys. Rev.* **29**, 466 (1927).

- [36] B. I. Stepanov, Universal relation between the absorption spectra and luminescence spectra of complex molecules, *Dokl. Akad. Nauk. SSSR+* **112**, 839 (1957).
- [37] L. P. Kazachenko and B. I. Stepanov, Mirror symmetry and the shape of absorption and luminescence bands of complex molecules, *Opt. Spektrosk.* **2**, 339 (1957).
- [38] D. E. McCumber, Einstein relations connecting broadband emission and absorption spectra, *Phys. Rev.* **136**, A954 (1964).
- [39] J. Klaers, The thermalization, condensation and flickering of photons, *J. Phys. B: At. Mol. Opt.* **47**, 243001 (2014).
- [40] E. A. Cornell and C. E. Wieman, Nobel lecture: Bose–Einstein condensation in a dilute gas, the first 70 years and some recent experiments, *Rev. Mod. Phys.* **74**, 875 (2002).
- [41] W. Ketterle, Nobel lecture: When atoms behave as waves: Bose–Einstein condensation and the atom laser, *Rev. Mod. Phys.* **74**, 1131 (2002).
- [42] M. D. Lee and C. W. Gardiner, Quantum kinetic theory. VI. The growth of a Bose-Einstein condensate, *Phys. Rev. A* **62**, 033606 (2000).
- [43] H. Deng, D. Press, S. Götzinger, G.S. Solomon, R. Hey, K.H. Ploog and Y. Yamamoto, Quantum degenerate exciton-polaritons in thermal equilibrium, *Phys. Rev. Lett.* **97**, 146402 (2006).
- [44] J. Kasprzak, D. D. Solnyshkov, R. Andre, L. S. Dang and G. Malpuech, Formation of an exciton polariton condensate: Thermodynamic versus kinetic regimes, *Phys. Rev. Lett.* **101**, 146404 (2008).
- [45] M. Wouters, I. Carusotto and C. Ciuti, Spatial and spectral shape of inhomogeneous nonequilibrium exciton-polariton condensates, *Phys. Rev. B* **77**, 115340 (2008).
- [46] J Schmitt, T Damm, D Dung, F Vewinger, J Klaers and M Weitz, Thermalization kinetics of light: From laser dynamics to equilibrium condensation of photons, *Phys. Rev. A* **92**, 011602 (2015).
- [47] Z. Hadzibabic, P. Krüger, M. Cheneau, B. Battelier and J. Dalibard, Berezinskii-Kosterlitz-Thouless crossover in a trapped atomic gas, *Nature* **441**, 1111 (2006).
- [48] P. Clade, C. Ryu, A. Ramanathan, K. Helmerson and W. D. Phillips, Observation of a 2d Bose gas: From thermal to quasicondensate to superfluid, *Phys. Rev. Lett.* **102**, 170401 (2009).
- [49] Z. Hadzibabic and J. Dalibard, Two-dimensional Bose fluids: An atomic physics perspective, *Lecture notes from the Varenna Summer School 23 June-3 July 2009. Published in Proceedings of the International School of Physics "Enrico Fermi", Course CLXXIII, "Nano optics and atomics: transport of light and matter waves", Editors R. Kaiser, D. Wiersma and L. Fallani. (IOS Press, Amsterdam and SIF, Bologna), 273 (2009).*
- [50] J. Klaers, J. Schmitt, T. Damm, F. Vewinger and M. Weitz, Bose-Einstein condensation of paraxial light, *Appl. Phys. B* **105**, 17 (2011).
- [51] K. Huang, Introduction to statistical physics, CRC Press, Boca Raton (2001).
- [52] R. M. Ziff, G. E. Uhlenbeck and M. Kac, Ideal Bose-Einstein gas, revisited, *Phys. Rep.* **32**, 169 (1977).
- [53] V. V. Kocharovskiy, V. V. Kocharovskiy, M. Holthaus, C. H. Raymond Ooi, A. A. Svidzinsky, W. Ketterle and M.O. Scully, Fluctuations in ideal and interacting Bose-Einstein condensates: From the laser phase transition analogy to squeezed states and bogoliubov quasiparticles, *Adv. Atom. Mol. Opt. Phy.* **53**, 291 (2006).

- [54] M. Fierz, Über die statistischen Schwankungen in einem kondensierenden System, *Helv. Phys. Acta* **29**, 47 (1955).
- [55] S. Grossmann and M. Holthaus, Microcanonical fluctuations of a Bose system's ground state occupation number, *Phys. Rev. E* **54**, 3495 (1996).
- [56] M. Holthaus, E. Kalinowski and K. Kirsten, Condensate fluktuations in trapped Bose gases: Canonical vs. microcanonical ensemble, *Ann. Phys. (N. Y.)* **270**, 198 (1998).
- [57] I. Fujiwara, D. ter Haar and H. Wergeland, Fluctuations in the population of the ground state of Bose systems, *J. Stat. Phys.* **2**, 329 (1970).
- [58] H. D. Politzer, Condensate fluctuations of a trapped, ideal Bose gas, *Phys. Rev. A* **54**, 5048 (1996).
- [59] P. Navez, D. Bitouk, M. Gajda, Z. Idziaszek and K. Rzazewski, Fourth statistical ensemble for the Bose-Einstein condensate, *Phys. Rev. Lett.* **79**, 1789 (1997).
- [60] S. Grossmann and M. Holthaus, Maxwell's demon at work: Two types of Bose condensate fluctuations in power-law traps, *Opt. Express* **1**, 262 (1997).
- [61] C. Weiss and M. Wilkens, Particle number counting statistics in ideal Bose gases, *Opt. Express* **1**, 272 (1997).
- [62] C. Weiss, S. Page and M. Holthaus, Factorising numbers with a Bose-Einstein condensate, *Physica A* **341**, 586 (2004).
- [63] M. O. Scully and W. E. Lamb, Quantum theory of an optical maser. i. General theory, *Phys. Rev.* **159**, 208 (1967).
- [64] J. Schmitt, T. Damm, D. Dung, F. Vewinger, J. Klaers and M. Weitz, Observation of grand-canonical number statistics in a photon Bose-Einstein condensate, *Phys. Rev. Lett.* **112**, 030401 (2014).
- [65] C. Ciuti, Statistical flickers in a Bose-Einstein condensate of photons, *Physics* **7**, 7 (2014).